

Detection of supernova neutrinos at spallation neutron sources^{*}

Huang Ming-Yang^{1,2;1)} GUO Xin-Heng^{3;2)} YOUNG Bing-Lin^{4,5;3)}

¹ Institute of High Energy Physics (IHEP), Chinese Academy of Sciences (CAS), Beijing 100049, China

² Dongguan Institute of Neutron Science (DINS), Dongguan 523808, China

³ College of Nuclear Science and Technology, Beijing Normal University, Beijing 100875, China

⁴ Department of Physics and Astronomy, Iowa State University, Ames, Iowa 5001, USA

⁵ Institute of Theoretical Physics, Chinese Academy of Sciences, Beijing, China

Abstract:

After considering the supernova shock effects, the Mikheyev-Smirnov-Wolfenstein effects, the neutrino collective effects, and the Earth matter effects, the detection of supernova neutrinos at China Spallation Neutron Sources is studied and the event numbers of different flavor supernova neutrinos observed through various reaction channels are calculated with the neutrino energy spectra described by the Fermi-Dirac distribution and “beta fit” distribution respectively. Furthermore, the numerical calculation method of supernova neutrino detection on the Earth is applied to some other spallation neutron sources, and the total event numbers of supernova neutrinos observed through different reactions channels are given.

Key words: neutron source, supernova neutrinos, neutrino effects, event number

PACS: 14.60.Pq, 25.30.Pt, 26.30.-k

1 Introduction

Supernovas (SNs) are extremely powerful explosions in the universe which terminate the life of some stars. They make the catastrophic end of stars more massive than eight solar masses ($> 8M_{\odot}$), leaving behind compact remnants such as neutron stars or black holes. The SN explosion is one of the most spectacular cosmic events and a source of new physical ideas [1]. A broad area of fundamental physics can be studied by the observation of SN [2]. Detection of SN neutrinos on the Earth [3], such as SN1987A [4, 5], has been a subject of intense investigation in astroparticle physics. Some information about the SN explosion mechanism and neutrino mixing parameters can be obtained by detecting SN neutrinos on the Earth [2, 6].

China Spallation Neutron Source (CSNS) [7] is a high power accelerator based facility. It consists of an 80 MeV proton linac, a 1.6 GeV Rapid Cycling Synchrotron (RCS), a solid tungsten target station, and instruments for spallation neutron applications [8]. The accelerator operates at 25 HZ repetition rate with an initial design beam power of 100 kW and is upgradeable to 500 kW [9, 10]. As the exclusive spallation neutron source in developing countries, CSNS will be among the top four of such facilities in the world until completion.

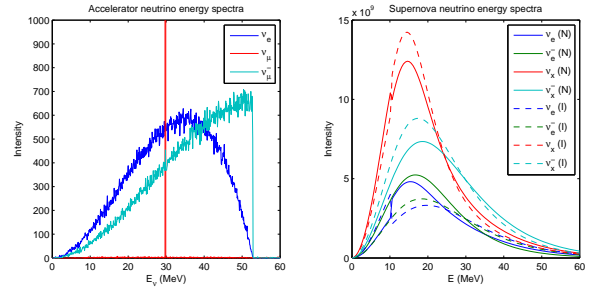


Fig. 1. Neutrino energy spectra. (a) accelerator neutrinos at CSNS; (b) SN neutrinos on the Earth. $N(I)$ corresponds to the normal (inverted) mass hierarchy, and $x = \mu, \tau$.

By using the code FLUKA, the processes of accelerator neutrinos production during the proton beam hitting on the tungsten target at CSNS were simulated, and the energy spectra of accelerator neutrinos were gained [11], as shown in Fig. 1(a). While considering the SN shock effects [12–15], the Mikheyev-Smirnov-Wolfenstein (MSW) effects [16–19], the neutrino collective effects [20–22], and the Earth matter effects [23–25], the detection of SN neutrinos on the Earth was studied [26]. Then, the energy spectra of SN neutrinos can be calculated, as shown in Fig. 1(b). To compare the energy spectra of accelerator neutrinos with that of SN neutrinos, it is clear that the energy spectrum ranges of SN neutrinos

^{*} Supported by National Natural Science Foundation of China (11205185, 11175020, 11275025, and 11575023)

1) E-mail: huangmy@ihep.ac.cn

2) E-mail: xhguo@bnu.edu.cn

3) E-mail: young@iastate.edu

are very close to that of accelerator neutrinos. Therefore, by using the accelerator neutrino detector at spallation neutron sources, different flavor neutrinos from a SN explosion can also be detected, and then can be served as a SN Early Warning System [27].

2 SN neutrino detection at CSNS

In the core collapse of SN, a vast amount of neutrinos are produced in two bursts [28, 29]. When SN neutrinos of each flavor are produced, they are approximately the effective mass eigenstates due to the extremely high matter density environment. While neutrinos propagate outward to the surface of the SN, they could be subjected to the SN shock effects, the MSW effects, and the neutrino collective effects. Then, after travelling the cosmic distance to reach the Earth, they go through a part of the Earth and are subjected to the Earth matter effects. Fig. 2 shows the path of SN neutrinos reaching the detector on the Earth.

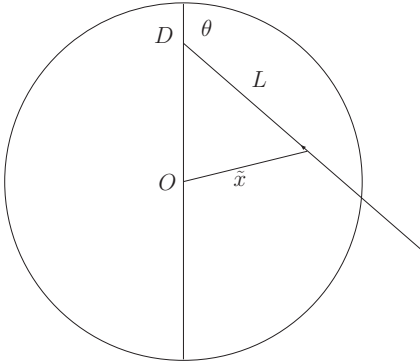


Fig. 2. Illustration of the path of SN neutrinos reaching the detector in the Earth. D is the location of the detector, θ is the incident angle of neutrinos, O is the center of the Earth, L is the distance neutrinos travel through the Earth, and \hat{x} is the distance of neutrinos to the center of the Earth.

When all effects, including the SN shock effects, the MSW effects, the neutrino collective effects, and the Earth matter effects, are taken into account, the SN neutrino fluxes at the detector can be written as [26]

$$\begin{aligned} F_{\nu_e}^D &= pF_{\nu_e}^{(0)} + (1-p)F_{\nu_x}^{(0)}, \\ F_{\bar{\nu}_e}^D &= \bar{p}F_{\bar{\nu}_e}^{(0)} + (1-\bar{p})F_{\bar{\nu}_x}^{(0)}, \\ 2F_{\nu_x}^D &= (1-p)F_{\nu_e}^{(0)} + (1+p)F_{\nu_x}^{(0)}, \\ 2F_{\bar{\nu}_x}^D &= (1-\bar{p})F_{\bar{\nu}_e}^{(0)} + (1+\bar{p})F_{\bar{\nu}_x}^{(0)}, \end{aligned} \quad (1)$$

where $x = \mu, \tau$, and the survival probabilities p and \bar{p} are given by

$$\begin{aligned} p &= P_{2e}[P_H P_{\nu\nu} + (1-P_H)(1-P_{\nu\nu})], \\ \bar{p} &= (1-\bar{P}_{2e})\bar{P}_{\nu\nu}, \end{aligned} \quad (2)$$

for the normal mass hierarchy and

$$\begin{aligned} p &= P_{2e}P_{\nu\nu}, \\ \bar{p} &= (1-\bar{P}_{2e})[\bar{P}_H\bar{P}_{\nu\nu} + (1-\bar{P}_H)(1-\bar{P}_{\nu\nu})], \end{aligned} \quad (3)$$

for the inverted mass hierarchy. In Eqs. (2) and (3), $P_{2e}(\bar{P}_{2e})$ is the probability that a (anti)neutrino mass eigenstate $\nu_2(\bar{\nu}_2)$ enters the surface of the Earth and arrives at the detector as an electron (anti)neutrino $\nu_e(\bar{\nu}_e)$, $P_{\nu\nu}(\bar{P}_{\nu\nu})$ is the probability that the (anti)neutrino $\nu(\bar{\nu})$ remains as $\nu(\bar{\nu})$ after the collective effects, and $P_H(\bar{P}_H)$ is the crossing probability for (anti)neutrinos to jump from one eigenstate to another at the high resonance layer [26].

We assume a “standard” SN explosion at a distance $D = 10$ kpc from the Earth, releasing a total energy $E_B = 3 \times 10^{53}$ erg (similar to SN1987A [4, 5]). For the SN neutrino of flavor α ($\alpha = e, \mu, \tau$), the luminosity flux is distributed in time as

$$L_\alpha(t) = \frac{E_B}{18} \exp(-t/3). \quad (4)$$

In general simulations, the time-integrated neutrino energy spectra can be described by the Fermi-Dirca distribution (the “Livermore” model) [30] or “beta fit” distribution (the “Garching” model) [31]:

(1) Fermi-Dirca distribution

$$F_\alpha^{(0)}(E) = \frac{L_\alpha(t)}{F_{\alpha 3} T_\alpha^4} \frac{E^2}{\exp(E/T_\alpha - \eta_\alpha) + 1}, \quad (5)$$

where E is the neutrino energy, T_α is the temperature of the neutrino α , η_α is the dimensionless pinching parameter of the spectrum, and $F_{\alpha j}$ is defined by

$$F_{\alpha j} = \int_0^\infty \frac{x^j}{\exp(x - \eta_\alpha) + 1} dx,$$

where j is an integer. The spectra obtained from numerical simulations can be well fitted by [32, 33]

$$\begin{aligned} T_{\nu_e} &= 3 - 4 \text{ MeV}, & \eta_{\nu_e} &\approx 3 - 5, \\ T_{\bar{\nu}_e} &= 5 - 6 \text{ MeV}, & \eta_{\bar{\nu}_e} &\approx 2.0 - 2.5, \\ T_{\nu_x} &= T_{\bar{\nu}_x} = 7 - 9 \text{ MeV}, & \eta_{\nu_x} &= \eta_{\bar{\nu}_x} \approx 0 - 2. \end{aligned} \quad (6)$$

(2) “Beta fit” distribution

$$\begin{aligned} F_\alpha^{(0)}(E) &= \frac{L_\alpha(t)}{\langle E_\alpha \rangle^2} \frac{\beta_\alpha^{\beta_\alpha}}{\Gamma(\beta_\alpha)} \left(\frac{E_\alpha}{\langle E_\alpha \rangle} \right)^{\beta_\alpha - 1} \\ &\quad \times \exp\left(-\beta_\alpha \frac{E_\alpha}{\langle E_\alpha \rangle}\right), \end{aligned} \quad (7)$$

where $\langle E_\alpha \rangle$ is the neutrino average energy and β_α is the dimensionless pinching parameter. The spectra obtained from numerical simulations can be well fitted by [2, 34]

$$\begin{aligned} \langle E_{\nu_e} \rangle &= \langle E_{\bar{\nu}_e} \rangle = 12 \sim 15 \text{ MeV}, \\ \langle E_{\nu_x} \rangle &= \langle E_{\bar{\nu}_x} \rangle = 15 \sim 18 \text{ MeV}, & \beta_\alpha &= 3.5 \sim 6. \end{aligned} \quad (8)$$

Therefore, the event numbers $N(i)$ of SN neutrinos observed through various reaction channels “ i ” can be calculated by

$$N(i) = N_T \int dE \cdot \sigma(i) \cdot \frac{1}{4\pi D^2} \cdot F_\alpha^D, \quad (9)$$

where N_T is the target number, $\sigma(i)$ is the cross section of the given reaction channel, and D is the distance between the SN and the Earth.

For CSNS [11], a medium scale detector would be placed just below the ground surface about 50-60 meters from the spallation target. A spherical 803 tons fiducial mass of mineral oil (CH_2 , density 0.845 g/cm^3) has a fiducial radius of 6.1 m, occupying a volume of 950 m^3 . Then the total event numbers of target protons, electrons, and ^{12}C are

$$\begin{aligned} N_T^{(p)} &= 6.90 \times 10^{31}, & N_T^{(e)} &= 2.76 \times 10^{32}, \\ N_T^{(C)} &= 3.45 \times 10^{31}. \end{aligned}$$

Table 1. Reaction channels used to detect SN neutrinos at CSNS, where E_{th} is the reaction threshold, the unit of E is MeV, and the cross sections for the ^{12}C reactions are the average cross sections.

Reaction	Equation	E_{th} (MeV)	Target numbers	Cross sections (cm^2)
$\bar{\nu}_e p$	$\bar{\nu}_e + p \rightarrow e^+ + n$	1.8	6.9×10^{31}	$9.5 \times 10^{-44} (E - 1.29)^2$
νe^-	$\nu_e + e^- \rightarrow \nu_e + e^-$	0	2.76×10^{32}	$9.20 \times 10^{-45} E$
	$\bar{\nu}_e + e^- \rightarrow \bar{\nu}_e + e^-$	0	2.76×10^{32}	$3.83 \times 10^{-45} E$
	$\nu_x + e^- \rightarrow \nu_x + e^-$	0	2.76×10^{32}	$1.57 \times 10^{-45} E$
	$\bar{\nu}_x + e^- \rightarrow \bar{\nu}_x + e^-$	0	2.76×10^{32}	$1.29 \times 10^{-45} E$
$\nu^{12}\text{C}$	$\nu_e + ^{12}\text{C} \rightarrow ^{12}\text{N} + e^-$	17.34	3.45×10^{31}	1.85×10^{-43}
	$\bar{\nu}_e + ^{12}\text{C} \rightarrow ^{12}\text{B} + e^+$	14.39	3.45×10^{31}	1.87×10^{-42}
	$\nu_e + ^{12}\text{C} \rightarrow ^{12}\text{C}^* + \nu'_e$	15.11	3.45×10^{31}	1.33×10^{-43}
	$\bar{\nu}_e + ^{12}\text{C} \rightarrow ^{12}\text{C}^* + \bar{\nu}'_e$	15.11	3.45×10^{31}	6.88×10^{-43}
	$\nu_x + ^{12}\text{C} \rightarrow ^{12}\text{C}^* + \nu'_x$	15.11	3.45×10^{31}	3.73×10^{-42}
	$\bar{\nu}_x + ^{12}\text{C} \rightarrow ^{12}\text{C}^* + \bar{\nu}'_x$	15.11	3.45×10^{31}	3.73×10^{-42}

It is clear that there are three reaction channels which can be used to detect SN neutrinos: the inverse beta decay, the neutrino-electron reactions, and the neutrino-carbon reactions. Table 1 shows the reaction thresholds, target numbers, and effective cross sections for the three reactions [35–38]. It can be seen that, for the inverse beta decay, the neutrino events can be identified by the detection of both the e^+ and the 2.2 MeV γ from the reaction $n + p \rightarrow d + \gamma$ with a mean capture time $\tau = 250 \mu\text{s}$ [39, 40]; for the neutrino-electron reactions, the neutrino events can be identified by the signal of the recoil electrons which are strong peaked along the neutrino direction, and this forward peaking is usually used for experiments to distinguish the electron elastic scattering from the neutrino reactions on nuclei [41, 42]; for the neutrino reactions on ^{12}C , there are two charged-current and six neutral-current reactions:

Charged-current capture of ν_e :

$$\begin{aligned} \nu_e + ^{12}\text{C} &\rightarrow ^{12}\text{N} + e^-, & E_{th} &= 17.34 \text{ MeV}, \\ ^{12}\text{N} &\rightarrow ^{12}\text{C} + e^+ + \nu_e, & \tau_{1/2} &= 11.00 \text{ ms}. \end{aligned}$$

Charged-current capture of $\bar{\nu}_e$:

$$\begin{aligned} \bar{\nu}_e + ^{12}\text{C} &\rightarrow ^{12}\text{B} + e^+, & E_{th} &= 14.39 \text{ MeV}, \\ ^{12}\text{B} &\rightarrow ^{12}\text{C} + e^- + \bar{\nu}_e, & \tau_{1/2} &= 20.20 \text{ ms}. \end{aligned}$$

Neutral-current inelastic scattering of ν_α or $\bar{\nu}_\alpha$ ($\alpha =$

e, μ, τ):

$$\begin{aligned} \nu_\alpha (\bar{\nu}_\alpha) + ^{12}\text{C} &\rightarrow ^{12}\text{C}^* + \nu'_\alpha (\bar{\nu}'_\alpha), & E_{th} &= 15.11 \text{ MeV}, \\ ^{12}\text{C}^* &\rightarrow ^{12}\text{C} + \gamma. \end{aligned}$$

The charged-current events have the delayed coincidence of a β decay following the interaction. The neutral-current events have a monoenergetic γ ray at 15.11 MeV. Therefore, the charged-current and neutral-current reactions on carbon can be tagged and observed by the neutrino detector [35, 43].

In Table 1, for the neutrino-carbon reactions, the effective cross sections of the charged-current interaction are given for SN neutrinos without oscillations. When neutrino oscillations are taken into account, the oscillations of higher energy ν_x into ν_e result in an increasing event rate since the expected ν_e energies are just at or below the reaction threshold. This leads to an increase by a factor of 35 for the efficiency cross section $\langle \sigma(^{12}\text{C}(\nu_e, e^-)^{12}\text{N}) \rangle$. Similarly, the efficiency cross section $\langle \sigma(^{12}\text{C}(\bar{\nu}_e, e^+)^{12}\text{B}) \rangle$ increases by a factor of 5.

Since the energy spectrum ranges of accelerator neutrinos and reactor neutrinos are close to that of SN neutrinos, the background due to the accelerator neutrinos from CSNS and the reactor neutrinos from Daya Bay reactor need to be estimated while observing SN neutrinos. After careful calculation and analysis [11], with the neutrino detector at CSNS, the event number of accelerator neutrinos which can be observed is about $10^{-3} \sim 10^{-4}$

per second. The neutrino luminosity of Daya Bay reactor is very large [44], however, due to the long distance of Daya Bay reactor from CSNS (about 70 km), the event number of reactor neutrinos observed at CSNS is about $10^{-3} \sim 10^{-4}$ per second by detailed calculation. It is known that the SN explosion lasts for only about 20 second. Therefore, the event numbers of accelerator neutrinos and reactor neutrinos are very few and can be ignored during the detection of SN neutrinos at CSNS.

SN relic neutrinos, also known as diffuse SN neutrino background, is of intense interest in neutrino astronomy and neutrino physics [45]. With the neutrino detector at CSNS, the event number of SN relic neutrinos which can be observed [46] is about $10^{-7} \sim 10^{-8}$ per second. Due to the very short time of SN explosion, the background of SN relic neutrinos can also be neglected.

In general, there is no serious background because of the characteristics of the SN neutrino events which are

concentrated in a short 20 second interval with energies no more than 30 MeV. This has been confirmed in the Kamiokande [4] and IMB [5] neutrino events of SN1987A.

In order to calculate the event numbers of SN neutrinos more accurately, the energy resolution and event selection need to be studied, and then the detector efficiency can be obtained. For the proposed CSNS detector, we choose to use the detector efficiency ε_{pc} for the inverse beta decay, ε_{ec} for the neutrino-electron reactions, ε_{cc} for the neutrino-carbon reactions, respectively, during the calculation of the SN neutrino event numbers [47].

To make use of the latest experiment results of neutrino oscillations [48, 49], the neutrino mixing parameters are given:

$$\Delta m_{21}^2 = 7.5 \times 10^{-5} eV^2, \quad |\Delta m_{32}^2| = 2.4 \times 10^{-3} eV^2, \\ \sin^2 \theta_{12} = 0.308, \quad \sin^2 \theta_{23} = 0.446, \quad \sin^2 \theta_{13} = 0.0237.$$

Table 2. Summary of the event number ranges of different flavor SN neutrinos detected in various reaction channels at CSNS. “Range (FD)” (“Range (BF)”) stands for the event number ranges of SN neutrinos calculated by using the Fermi-Dirac (“beta fit”) distribution, “[x, y] ε ” stands for the event number range satisfied $x \times \varepsilon \leq N \leq y \times \varepsilon$ where ε is the detector efficiency.

Hierarchy	Reaction	Flavor	Range (FD)	Range (BF)
Normal	$\bar{\nu}_e p$	$\bar{\nu}_e$	[370.81, 512.94] ε_{pc}	[221.15, 316.95] ε_{pc}
	νe^-	ν_e	[6.36, 6.72] ε_{ec}	[6.62, 6.73] ε_{ec}
		$\bar{\nu}_e$	[2.76, 2.83] ε_{ec}	[2.81, 2.83] ε_{ec}
		ν_x	[2.34, 2.40] ε_{ec}	[2.33, 2.35] ε_{ec}
		$\bar{\nu}_x$	[1.91, 1.93] ε_{ec}	[1.91, 1.92] ε_{ec}
	$\nu^{12}C$	ν_e	[21.69, 34.53] ε_{cc}	[41.52, 52.35] ε_{cc}
		$\bar{\nu}_e$	[16.61, 25.15] ε_{cc}	[29.74, 37.29] ε_{cc}
		ν_x	[13.48, 20.01] ε_{cc}	[23.68, 28.08] ε_{cc}
		$\bar{\nu}_x$	[18.99, 28.13] ε_{cc}	[34.00, 41.11] ε_{cc}
Inverted	$\bar{\nu}_e p$	$\bar{\nu}_e$	[446.31, 640.79] ε_{pc}	[255.22, 354.61] ε_{pc}
	νe^-	ν_e	[6.86, 7.21] ε_{ec}	[6.92, 7.08] ε_{ec}
		$\bar{\nu}_e$	[2.85, 2.87] ε_{ec}	[2.84, 2.85] ε_{ec}
		ν_x	[2.25, 2.31] ε_{ec}	[2.28, 2.30] ε_{ec}
		$\bar{\nu}_x$	[1.89, 1.90] ε_{ec}	[1.90, 1.91] ε_{ec}
	$\nu^{12}C$	ν_e	[28.77, 41.21] ε_{cc}	[49.20, 58.91] ε_{cc}
		$\bar{\nu}_e$	[33.10, 48.19] ε_{cc}	[58.52, 70.33] ε_{cc}
		ν_x	[11.35, 17.21] ε_{cc}	[21.13, 25.45] ε_{cc}
		$\bar{\nu}_x$	[14.55, 21.15] ε_{cc}	[25.85, 31.32] ε_{cc}

By using Eqs. (1)-(9), the event numbers of SN neutrinos detected on the Earth can be calculated. The numerical results calculated with the neutrino energy spectra described by the Fermi-Dirac distribution and “beta fit” distribution are both shown in Table 2. In the table, the event number ranges of different flavor neutrinos observed through various reaction channels: the inverse beta decay, the neutrino-electron reactions, and the neutrino-carbon reactions, are given. It can be found that:

(i) If $\varepsilon_{pc} \simeq \varepsilon_{ec} \simeq \varepsilon_{cc}$, the total event number of differ-

ent flavor neutrinos observed through the channel of the neutrino-electron reactions is much smaller than that of the inverse beta decay and neutrino-carbon reactions;

(ii) If $\varepsilon_{pc} \simeq \varepsilon_{ec} \simeq \varepsilon_{cc}$, the event number of $\bar{\nu}_e$ observed through the channel of the inverse beta decay is much larger than that of the neutrino-electron reactions and neutrino-carbon reactions;

(iii) For the inverse beta decay, the event number of $\bar{\nu}_e$ calculated with the neutrino energy spectra described by the Fermi-Dirac distribution is larger than that by the “beta fit” distribution; however, for the neutrino-carbon

reactions, the event numbers of different flavor neutrinos calculated with the neutrino energy spectra described by the Fermi-Dirac distribution are all smaller than that by the “beta fit” distribution;

(iv) For the neutrino-electron reactions and neutrino-carbon reactions, the event numbers of ν_e and $\bar{\nu}_e$ are larger than that of ν_x and $\bar{\nu}_x$;

(v) More precise values of T_α and η_α ($\langle E_\alpha \rangle$ and β_α) will help obtain more reliable event number ranges of SN neutrinos [1, 50].

(vi) Until the completion of the design of neutrino detector at CSNS, the detector efficiency will be given and more accurate event number ranges of SN neutrinos can be gained.

In the next section, the numerical calculation method of SN neutrino detection on the Earth will be applied for some other spallation neutron sources at GeV energy range in the world.

3 SN neutrino detection at other spallation neutron sources

Table 3. Summary of the proposed neutrino detectors at some current spallation neutron sources at GeV energy range.

Detector	Material	Mass (kton)	Depth (km)	Target numbers
ν SNS [58]	CH ₂	0.886	0.006	$N_p: 7.62 \times 10^{31}$
				$N_e: 3.05 \times 10^{32}$
				$N_C: 3.81 \times 10^{31}$
ν ESS [59]	H ₂ O	500	1.0	$N_p: 3.35 \times 10^{34}$
				$N_e: 1.67 \times 10^{35}$
				$N_O: 1.67 \times 10^{34}$

In the history of neutrino research, there are many famous neutrino experiments which were based on spallation neutron sources and gained very important achievements [51], such as the Liquid Scintillator Neutrino Detector (LSND) [52] at the Los Alamos Meson Physics Facility (LAMPF), the Karlsruhe Rutherford Medium Energy Neutrino experiment (KARMEN) [53, 54] at the Spallation Neutron Source of Rutherford Appleton Laboratory (ISIS) [55] and so on. Since the 21st century, some new spallation neutron sources have been finished or under construction, and they may be used for accelerator neutrino experiments in the future, such as the Spallation Neutron Source at Oak Ridge National Laboratory (SNS) [56], CSNS [7], the European Spallation Neutron Source (ESS) [57] and so on. In Table 3, we list the material of liquid scintillator, the detector masses, the underground depth of the detectors, and the target numbers of the proposed neutrino detectors at some current spallation neutron sources at GeV energy range in the world. Similar to the proposed neutrino detector at

CSNS discussed in the above section, these neutrino detectors can also be used for observing SN neutrinos, and some information about the neutrino mixing parameters and explosion mechanism of SN may be gained.

For the neutrino detector at SNS, there are three reaction channels which can be used to detect SN neutrinos: the inverse beta decay, the neutrino-electron reactions, and the neutrino-carbon reactions, and their effective cross sections are given in Table 1. For the neutrino detector at ESS, there are also three reaction channels which can be used to detect SN neutrinos: the inverse beta decay, the neutrino-electron reactions, and the neutrino-oxygen reactions. The effective cross sections for the inverse beta decay and neutrino-electron reactions are given in Table 1, and the total effective cross sections for the neutrino-oxygen reactions are given as follows [60–62]:

$$\begin{aligned}
 \langle \sigma(^{16}\text{O}(\nu_e, e^-)^{16}\text{F}^*) \rangle &= 1.91 \times 10^{-43} \text{cm}^2, \\
 \langle \sigma(^{16}\text{O}(\bar{\nu}_e, e^+)^{16}\text{N}^*) \rangle &= 1.05 \times 10^{-42} \text{cm}^2, \\
 \langle \sigma(^{16}\text{O}(\nu_x, \nu'_x)^{16}\text{O}^*) \rangle &= 5.90 \times 10^{-42} \text{cm}^2, \\
 \langle \sigma(^{16}\text{O}(\bar{\nu}_x, \bar{\nu}'_x)^{16}\text{O}^*) \rangle &= 4.48 \times 10^{-42} \text{cm}^2.
 \end{aligned} \tag{10}$$

The effective cross sections of the charged-current interaction in Eq. (10) are given for SN neutrinos without oscillations. When neutrino oscillations are taken into account, the oscillations of higher energy ν_x into ν_e result in an increased event rate since the expected ν_e energies are just at or below the reaction threshold. This leads to an increase by a factor of 71.7 for the efficiency cross section $\langle \sigma(^{16}\text{O}(\nu_e, e^-)^{16}\text{F}^*) \rangle$. Similarly, the efficiency cross section $\langle \sigma(^{16}\text{O}(\bar{\nu}_e, e^+)^{16}\text{N}^*) \rangle$ is growing by a factor of 9.2.

Similar to the CSNS detector, in order to calculate the event numbers of SN neutrinos more accurately, for the SNS detector, we choose to use the detector efficiency ε_{ps} for the inverse beta decay, ε_{es} for the neutrino-electron reactions, ε_{cs} for the neutrino-carbon reactions, respectively; for the ESS detector, we choose to use the detector efficiency ε_{pe} for the inverse beta decay, ε_{ee} for the neutrino-electron reactions, ε_{oe} for the neutrino-oxygen reactions, respectively.

By using Eqs. (1)-(9), the event numbers of SN neutrinos detected at SNS and ESS can be calculated. The numerical results calculated with the neutrino energy spectra described by the Fermi-Dirac distribution and “beta fit” distribution are both shown in Table 4. In the table, the total event number ranges of SN neutrinos observed through various reaction channels: the inverse beta decay, the neutrino-electron reactions, the neutrino-carbon reactions, and the neutrino-oxygen reactions, are given. It can be found that:

(i) If the efficiencies of different detectors are similar, then the total event number of SN neutrinos detected at ESS is much larger than that at CSNS and SNS;

(ii) The total event numbers of SN neutrinos detected in the case of inverted hierarchy are larger than that of normal hierarchy;

(iii) If the detector efficiencies of different reaction channels are similar, then the total event number of SN neutrinos observed through the channel of the neutrino-electron reactions is much smaller than that of the inverse beta decay, the neutrino-carbon reactions, and the neutrino-oxygen reactions;

(iv) For the inverse beta decay, the total event number of SN neutrinos calculated with the neutrino energy spectra described by the Fermi-Dirac distribution is larger than that by the “beta fit” distribution; however, for the neutrino-carbon reactions and neutrino-oxygen reactions, the total event numbers of SN neutrinos calculated with the neutrino energy spectra described by the Fermi-Dirac distribution are both smaller than that by the “beta fit” distribution.

Table 4. Summary of the total event number ranges of SN neutrinos detected in various reactions at SNS and ESS. “Range (FD)” (“Range (BF)”) stands for the event number ranges of SN neutrinos calculated by using the Fermi-Dirac (“beta fit”) distribution, “[x , y] ε ” stands for the event number range satisfied $x \times \varepsilon \leq N \leq y \times \varepsilon$ where ε is the detector efficiency.

Detector	Hierarchy	Reaction	Range (FD)	Range (BF)
ν SNS	Normal	$\bar{\nu}_e p$	$[410.21, 566.47]\varepsilon_{ps}$	$[244.33, 350.02]\varepsilon_{ps}$
		νe^-	$[14.88, 15.25]\varepsilon_{es}$	$[15.15, 15.26]\varepsilon_{es}$
		$\nu^{12}C$	$[79.13, 118.26]\varepsilon_{cs}$	$[142.95, 174.88]\varepsilon_{cs}$
	Inverted	$\bar{\nu}_e p$	$[493.13, 707.65]\varepsilon_{ps}$	$[281.85, 391.62]\varepsilon_{ps}$
		νe^-	$[15.39, 15.71]\varepsilon_{es}$	$[15.44, 15.58]\varepsilon_{es}$
		$\nu^{12}C$	$[97.02, 141.01]\varepsilon_{cs}$	$[170.92, 205.36]\varepsilon_{cs}$
ν ESS	Normal	$\bar{\nu}_e p$	$[1.80 \times 10^5, 2.49 \times 10^5]\varepsilon_{pe}$	$[1.07 \times 10^5, 1.54 \times 10^5]\varepsilon_{pe}$
		νe^-	$[8.15 \times 10^3, 8.35 \times 10^3]\varepsilon_{ee}$	$[8.30 \times 10^3, 8.35 \times 10^3]\varepsilon_{ee}$
		$\nu^{16}O$	$[4.73 \times 10^4, 7.18 \times 10^4]\varepsilon_{oe}$	$[8.72 \times 10^4, 1.07 \times 10^5]\varepsilon_{oe}$
	Inverted	$\bar{\nu}_e p$	$[2.17 \times 10^5, 3.11 \times 10^5]\varepsilon_{pe}$	$[1.24 \times 10^5, 1.72 \times 10^5]\varepsilon_{pe}$
		νe^-	$[8.43 \times 10^3, 8.61 \times 10^3]\varepsilon_{ee}$	$[8.45 \times 10^3, 8.53 \times 10^3]\varepsilon_{ee}$
		$\nu^{16}O$	$[5.89 \times 10^4, 8.56 \times 10^4]\varepsilon_{oe}$	$[1.04 \times 10^5, 1.25 \times 10^5]\varepsilon_{oe}$

4 Summary and discussion

In this paper, the SN neutrino detection on the Earth was studied. While considering all effects: the SN shock effects, the MSW effects, the neutrino collective effects, and the Earth matter effects, the detection of SN neutrinos on the Earth was studied. Then, the event number ranges of different flavor SN neutrinos observed through various reaction channels at CSNS: the inverse beta decay, the neutrino-electron reactions and the neutrino-carbon reactions, were calculated with the neutrino energy spectra described by the Fermi-Dirac distribution and “beta fit” distribution respectively.

Applying the numerical calculation method of SN neutrino detection on the Earth to some other spallation neutron sources (SNS and ESS) at GeV energy range, and the total event number ranges of SN neu-

trinos detected in different reactions channels (SNS: the inverse beta decay, the neutrino-electron reactions, the neutrino-carbon reactions; ESS: the inverse beta decay, the neutrino-electron reactions, the neutrino-oxygen reactions) were calculated.

In the future, after the completion of the design of neutrino detector at spallation neutron sources (CSNS, SNS, ESS), the detector efficiency will be given and more accurate event number ranges of SN neutrinos can be gained. Furthermore, it is known that more precise values of T_α and η_α ($\langle E_\alpha \rangle$ and β_α) will give more reliable event number ranges of SN neutrinos.

The authors would like to thank S. Wang and S.-J. Ding for helpful discussions and support.

References

- Mirizzi A, Tamborra I, Janka H T et al. Supernova Neutrinos: Production, Oscillations and Detection. arXiv: 1508.00785 [astro-ph.HE]
- Kotake K, Sato K, Takahashi K. Rept. Prog. Phys., 2006, **69**: 971C1143
- Guo X H, Huang M Y, Young B L. Chin. Phys. C, 2010, **34**: 257-261
- Hirata K, Kajita T, Koshiba M et al. Phys. Rev. Lett., 1987,

- 58:** 1490-1493
- 5 Bionta R M, Blewitt G, Bratton C B et al. Phys. Rev. Lett., 1987, **58:** 1494-1496
- 6 Scholberg K. Ann. Rev. Nucl.Part. Sci., 2012, **62:** 81-103
- 7 CSNS Project Team. China Spallation Neutron Source Feasibility Reaearch Report. Institute of High Energy Physics and Institute of Physics, Chinese Academy of Sciences, 2009 (in Chinese)
- 8 Wei J, Fu S N, Tang J Y et al. Chin. Phys. C, 2009, **33:** 1033-1042
- 9 Wang S, Fang S X, Fu S N et al. Chin. Phys. C, 2009, **33:** 1-3
- 10 Huang M Y, Wang S, Qiu J et al. Chin. Phys. C, 2013, **37:** 067001
- 11 Huang M Y. Study on accelerator neutrino detection at a spal-
lation source. arXiv: 1507.08765 [hep-ph]
- 12 Wilson J R. Numerical Astrophysics. Ed. Centrella J M, LeBlanc J M, Bowers R L, Boston, Jones and Bartlett, 1985. 422-434
- 13 Schirato R C, Fuller G M. Connection between supernova shocks, flavor transformation, and the neutrino signal. arXiv: 0205390 [astro-ph]
- 14 Hudepohl L, Muller B, Janka H T et al. Phys. Rev. Lett., 2010, **104:** 251101
- 15 Sarikas S, Raffelt G G, Hudepohl L et al. Phys. Rev. Lett., 2012, **108:** 061101
- 16 Wolfenstein L. Phys. Rev. D, 1978, **17:** 2369-2374
- 17 Mikheyev S P, Smirnov A Y. Sov. J. Nucl. Phys., 1985, **42:** 913-917
- 18 Kuo T K, Pantaleone J. Rev. Mod. Phys., 1989, **61:** 937-979
- 19 Blennow M, Smirnov A Y. Adv. High Energy Phys., 2013, **2013:** 972485
- 20 Dasgupta B, Dighe A, Mirizzi A. Phys. Rev. Lett., 2008, **101:** 171801
- 21 Duan H Y, Fuller G M, Carlson J. Comp. Scie. & Disc., 2008, **1:** 015007
- 22 Duan H Y, Fuller G M, Qian Y Z. Ann. Rev. Nucl. Part. Sci., 2010, **60:** 569-594
- 23 Dighe A S, Smirnov A Y. Phys. Rev. D, 2000, **62:** 033007
- 24 Ioannisian A N, Smirnov A Y. Phys. Rev. Lett., 2004, **93:** 241801
- 25 Guo X H, Huang M Y, Young B L. Phys. Rev. D, 2009, **79:** 113007
- 26 Huang M Y, Guo X H, Young B L. Phys. Rev. D, 2010, **82:** 033011
- 27 Antonioli P, Fienberg R T, Fleuret F et al. New J. Phys., 2004, **6:** 114
- 28 Giunti C, Kim C W. Fundamentals of Neutrino Physics and Astrophysics. New York: Oxford, 2007, 511-539
- 29 Mohapatra R N, Pal P B. Massive Neutrino in Physics and Astrophysics. Singapore, World Scientific, 2004, 340-358
- 30 Totani T, Sato K, Dalhed H E et al. Astrophys. J., 1998, **496:** 216-225
- 31 Keil M T, Raffelt G G, Janka H T. Astrophys. J., 2003, **590:** 971-991
- 32 Janka H T, Hillebrandt W. Astron. Astrophys., 1989, **224:** 49-56
- 33 Janka H T, Hillebrandt W. Astron. Astrophys. Suppl. Ser., 1989, **78:** 375-397
- 34 Chakraborty S, Choubey S, Goswami S et al. J. Cosmol. Astropart. Phys., 2010, **1006:** 007
- 35 Cadonati L, Calaprice F P, Chen M C. Astropart. Phys., 2002, **16:** 361-372
- 36 Arafune J, Fukugita M. Phys. Rev. Lett., 1987, **59:** 367-369
- 37 Fukugita M, Kohyama Y, Kubodera K. Phys Lett. B, 1988, **212:** 139-144
- 38 Kolbe E, Langanke K, Vogel P. Nucl. Phys. A, 1999, **652:** 91-100
- 39 Athanassopulos C, Auerbach L B, Bauer D A et al. Phys. Rev. Lett., 1995, **75:** 2650-2653
- 40 Athanassopulos C, Auerbach L B, Burman R L et al. Phys. Rev. C, 1996, **54:** 2685-2708
- 41 Allen R C, Chen H H, Doe P J et al. Phys. Rev. D, 1993, **47:** 11-28
- 42 Imlay R, VanDalen G J. J. Phys. G: Nucl. Part. Phys., 2003, **29:** 2647-2664
- 43 Auerbach L B, Burman R L, Caldwell D O et al. Phys. Rev. D, 2002, **66:** 015501
- 44 Daya Bay Collaboration. A Precision Measurement of the Neutrino Mixing Angle θ_{13} Using Reactor Antineutrinos at Daya Bay. arXiv: 0701029 [hep-ex]
- 45 Nakazato K. Phys. Rev. D, 2013, **88:** 083012
- 46 Zhang H, Abe K, Hayato Y et al. Astropart. Phys., 2015, **60:** 41-46
- 47 VanDalen G J. Oscillations and Cross Sections at the SNS with a Large Cerenkov Detector. arXiv: 0309014 [nucl-ex]
- 48 Olive K A, Agashe K, Amsler C et al. Chin. Phys. C, 2014, **38:** 090001
- 49 Gapozzi F, Fogli G L, Lisi E et al. Phys. Rev. D, 2014, **89:** 093018
- 50 Tamborra I, Raffelt G G, Hanke F et al. Phys. Rev. D, 2014 **90:** 045032
- 51 Burman R L, Louis W C. J. Phys. G: Nucl. Part. Phys., 2003, **29:** 2499-2512
- 52 Athanassopoulos C, Auerbach L B, Bauer D et al. Nucl. Instrum. Methods Phys. Res. A, 1997, **388:** 149-172
- 53 Drexlin G, Eberhard V, Gemmeke et al. Nucl. Instrum. Methods Phys. Res. A, 1990, **289:** 490-495
- 54 Burman R L, Dodd A C, Plischke P. Nucl. Instrum. Methods Phys. Res. A, 1996, **368:** 416-424
- 55 Boardman B. Spallation Neutron Source: Description of Accelerator and Target. RL-82-006, 1982
- 56 SNS Project Team. Spallation Neutron Source Design Manual. June, 1998
- 57 ESS Central Project Team. ESS Technical Design Report. ESS-doc-274-v15, 2015
- 58 Elnimr M, Stancu I, Yeh M et al. The OscSNS White Paper. arXiv:1307.7097 [physics.ins-det]
- 59 Baussan E, Blennow M, Bogomilov M et al. Nucl. Phys. B, 2014, **885:** 127-149
- 60 Kolbe E, Langanke K, Vogel P. Phys. Rev. D, 2002, **66:** 013007
- 61 Langanke K, Vogel P, Kolbe E. Phys. Rev. Lett., 1996, **76:** 2629-2632
- 62 Nussinov S, Shrock R. Phys. Rev. Lett., 2001, **86:** 2223-2226